Theory

Cell

Photoconversion and Nuclear Trafficking Cycles Determine Phytochrome A's Response Profile to Far-Red Light

Julia Rausenberger,[1,2,7] Anke Tscheuschler,[2] Wiebke Nordmeier,[5] Florian Wüst,[2] Jens Timmer,[3,4,6] Eberhard Schäfer,[2,4] Christian Fleck,[1,*] and Andreas Hiltbrunner[5,*]

[1]Centre for Biological Systems Analysis (ZBSA)
[2]Faculty of Biology
[3]Freiburg Institute for Advanced Studies (FRIAS)
[4]BIOSS Centre for Biological Signalling Studies
University of Freiburg, 79104 Freiburg, Germany
[5]Center for Plant Molecular Biology (ZMBP), University of Tübingen, 72076 Tübingen, Germany
[6]Department of Clinical and Experimental Medicine, Linköping University, SE-581 83 Linköping, Sweden
[7]Present address: School of Life Sciences, University of Applied Sciences Northwestern Switzerland, 4132 Muttenz, Switzerland
*Correspondence: christian.fleck@fdm.uni-freiburg.de (C.F.), andreas.hiltbrunner@zmbp.uni-tuebingen.de (A.H.)
DOI 10.1016/j.cell.2011.07.023

SUMMARY

Phytochrome A (phyA) is the only photoreceptor in plants, initiating responses in far-red light and, as such, essential for survival in canopy shade. Although the absorption and the ratio of active versus total phyA are maximal in red light, far-red light is the most efficient trigger of phyA-dependent responses. Using a joint experimental-theoretical approach, we unravel the mechanism underlying this shift of the phyA action peak from red to far-red light and show that it relies on specific molecular interactions rather than on intrinsic changes to phyA's spectral properties. According to our model, the dissociation rate of the phyA-FHY1/FHL nuclear import complex is a principle determinant of the phyA action peak. The findings suggest how higher plants acquired the ability to sense far-red light from an ancestral photoreceptor tuned to respond to red light.

INTRODUCTION

Light is an abiotic factor, which is particularly important for plants. It is used as a source of energy but also provides information about the environment. To monitor the intensity, quality, and direction of incident light, plants employ different types of photoreceptors, such as the phototropins and cryptochromes, which are blue light (B) receptors, or the red (R)/far-red (FR) light-absorbing phytochromes (Devlin et al., 2007). In *Arabidopsis*, there are five phytochromes (phyA-phyE), among which phyA and phyB are most important. PhyB is the dominating phytochrome species in light-grown and adult plants and plays a role in the shade avoidance response, regulation of flowering, and de-etiolation in R. In contrast, the switch from skotomorphogenic (development in the dark) to photomorphogenic (development in light) growth in FR-enriched environments requires phyA, which accumulates to very high levels in etiolated seedlings but is rapidly degraded upon irradiation with light (Bae and Choi, 2008).

Plant phytochromes are dimeric photoreceptors containing a covalently bound open-chain tetrapyrrole as chromophore (Rockwell et al., 2006). They have a photocycle with Pr as the ground state and Pfr as a longer-lived intermediate. Pr is biologically inactive and exhibits maximal absorption in R, whereas Pfr has an absorption peak in FR and is considered the active form of phytochromes. By absorption of light, they can reversibly interconvert between Pr and Pfr via short-lived photochemical intermediates (Mancinelli, 1994; Rockwell et al., 2006). Typically, phyB-mediated responses are induced by R and can be canceled by an FR pulse immediately following the R treatment (Casal et al., 2003). This mode of action, termed low fluence response (LFR), is consistent with a model in which phytochromes work as light switches that can be turned on and off by irradiation with R and FR. However, phyA-mediated responses are induced by very low amounts of light of any wavelength (very low fluence response [VLFR]) or by continuous irradiation with high fluence rate FR (high irradiance response [HIR]) and cannot be explained by a simple light switch (Casal et al., 2003). Although Pr and Pfr have absorption peaks at 667 nm (R) and 730 nm (FR), respectively, they absorb in FR and R as well. Thus, irradiation with either R or FR drives the conversion between Pr and Pfr in both directions. This results in continuous cycling between Pr and Pfr, which establishes the equilibrium between the two conformers depending on the wavelength, but not on the fluence rate (Mancinelli, 1994).

PhyA localizes to the cytosol in the dark and accumulates in the nucleus in response to irradiation with FR (Bae and Choi, 2008). Translocation of phyA into the nucleus is indispensable for FR perception and depends on the two functional homologs FHY1 and FHL, which physically interact with phyA (Hiltbrunner et al., 2005, 2006; Rösler et al., 2007; Shen et al., 2009; Yang

et al., 2009). The amount of phyA accumulating in the nucleus of FR-treated seedlings exceeds the total level of FHY1 and FHL that is available in a cell by several-fold. Therefore, FHY1/FHL have been predicted to work as shuttle proteins that cycle between the cytosol and the nucleus (Genoud et al., 2008).

PhyA is essential for de-etiolation in FR-rich environments, such as in canopy shade, and it may have provided an adaptive advantage to early angiosperms during colonization of habitats dominated by gymnosperms and ferns (Mathews, 2005). Although, as for any other phytochrome, the Pfr/Ptot ratio (Ptot = Pr + Pfr) is much higher in R than in FR, the action spectra for hypocotyl growth inhibition and other high irradiance responses (HIRs) exhibit a peak in the FR range of the spectrum (Figure S1 available online), which is absent in *phyA* mutant plants (Shinomura et al., 2000). Several models have been proposed to explain why maximal photon efficiency is shifted toward FR despite the lower relative abundance of the active Pfr form, but none link the shift to defined components or molecular events (Hennig et al., 1999, 2000; Schäfer, 1975; Shinomura et al., 2000). Interestingly, both HIRs and efficient accumulation of phyA in the nucleus require continuous irradiation with high fluence rate FR; thus, phyA nuclear transport itself can be considered an HIR.

In this work, we show that nucleocytoplasmic shuttling of FHY1/FHL plays a decisive role in phyA signaling and the HIR. Based on this finding, we develop a mathematical model for the HIR that integrates the current knowledge of phyA dynamics, nuclear transport, and interaction with FHY1/FHL. Our investigation shows that the dynamic model of the phyA interaction network intrinsically exhibits the typical features of the HIR and that the principle mechanism underlying the R→FR shift of the peak in the phyA action spectrum can be understood in simple, molecular terms. Finally, the model presented in this report also offers an explanation for the difference in spectral responsiveness of phyA and phyB despite the fact that they have identical photophysical properties.

RESULTS

Interaction with phyA Slows Down FHY1 Nucleocytoplasmic Shuttling

FHY1/FHL have been predicted to shuttle between the cytosol and the nucleus in order to transport more than only one phyA per FHY1/FHL (Genoud et al., 2008). We tested this using fluorescence recovery after photobleaching (FRAP) and fluorescence loss in photobleaching (FLIP) assays to analyze the mobility of yellow fluorescent protein (YFP)-tagged FHY1 in etiolated *Arabidopsis* seedlings. These approaches showed that YFP-FHY1 is indeed highly mobile and moves in both directions between the cytosol and the nucleus (Figures 1A and 1B). Interestingly, the mobility of YFP-FHY1 was strongly reduced in seedlings, which had been irradiated for 5 min with R to establish high levels of Pfr, whereas a 5 min R treatment did not affect the YFP-FHY1 mobility in the absence of phyA (Figures 1C and 1D).

Pfr Is Essential for phyA Nuclear Transport

In FR (730 nm), only about 2% of the total phyA is in Pfr (Mancinelli, 1994). Nevertheless, under these conditions, seedlings accumulate high levels of phyA in the nucleus, which account for much more than only 2% of the total phyA. This suggests that, in seedlings grown in FR, the major part of phyA in the nucleus is in Pr. However, phyA C323A, which is unable to bind the chromophore and cannot be converted to Pfr (Rockwell et al., 2006) (see Supplemental Information), did not accumulate in the nucleus of *phyA* mutant seedlings, and in yeast two-hybrid assays, it did not interact with FHY1 (Figure 2A and Figure S2). Thus, we conclude that only Pfr can translocate from the cytosol into the nucleus and that all nuclear-localized Pr results from photoconversion of phyA, which has been transported as Pfr.

Constitutively Active phyA Blocks phyA Nuclear Transport

Recently, Su and Lagarias (2007) described a phyB mutant (Y276H), which is constitutively active. Dark-grown seedlings expressing phyB Y276H exhibited a constitutively photomorphogenic (*cop*) phenotype and resembled de-etiolated wild-type seedlings at the transcriptome level (Hu et al., 2009; Su and Lagarias, 2007). PhyA Y242H-YFP contains a Y-to-H amino acid substitution at position 242, which corresponds to the amino acid change in the phyB Y276H mutant. Expression of phyA Y242H-YFP in wild-type background resulted in a *cop* phenotype as well, which was, however, much less pronounced than in seedlings expressing phyB Y276H (Su and Lagarias, 2007; Figure 3A and Figure S3). qPCR analyses showed that light-induced genes, such as PRR9 or CAB2, are upregulated (PRR9, 3.4-fold; CAB2, 7.0-fold) in dark-grown wild-type seedlings containing phyA Y242H-YFP (Figures 3C and 3D). Interestingly, phyA Y242H-YFP still depends on FHY1/FHL for activity, as *fhy1 fhl* seedlings expressing phyA Y242H-YFP remained fully etiolated (Figure S3).

In FR, the expression of phyA Y242H-YFP resulted in a strong dominant-negative phenotype (Figures 3A and 3B), which is in agreement with data by Su and Lagarias (2007) but is nevertheless not easy to reconcile with the idea that phyA Y242H-YFP is a constitutively active photoreceptor. Yet, consistent with this finding, phyA Y242H-YFP partially suppressed the upregulation of PRR9 and CAB2 in seedlings exposed to light (Figures 3C and 3D). An important prediction of the FHY1 shuttling model suggested by Genoud et al. (2008) is that any mutation that interferes with FHY1 recycling should interfere with nuclear transport of phyA and, as a consequence, result in reduced sensitivity to FR. The FRAP/FLIP experiments with YFP-FHY1 indicate that high levels of Pfr decrease the mobility of FHY1 (Figure 1). As phyA Y242H-YFP-expressing plants contain high amounts of "Pfr," nuclear transport of phyA Y242H-YFP may be reduced. Using fluorescence microscopy, we found that only very low levels of phyA Y242H-YFP accumulate in the nucleus, irrespective of whether or not the seedlings were exposed to light (Figure 3E). Moreover, in seedlings coexpressing phyA Y242H-YFP and cyan fluorescent protein (CFP)-tagged wild-type phyA, the "constitutively active" phyA inhibited nuclear transport of phyA-CFP (Figure 3E). As phyA nuclear transport is required for FR signaling (Hiltbrunner et al., 2006; Rösler et al., 2007), these findings can explain the dominant-negative effect of phyA Y242H-YFP in FR.

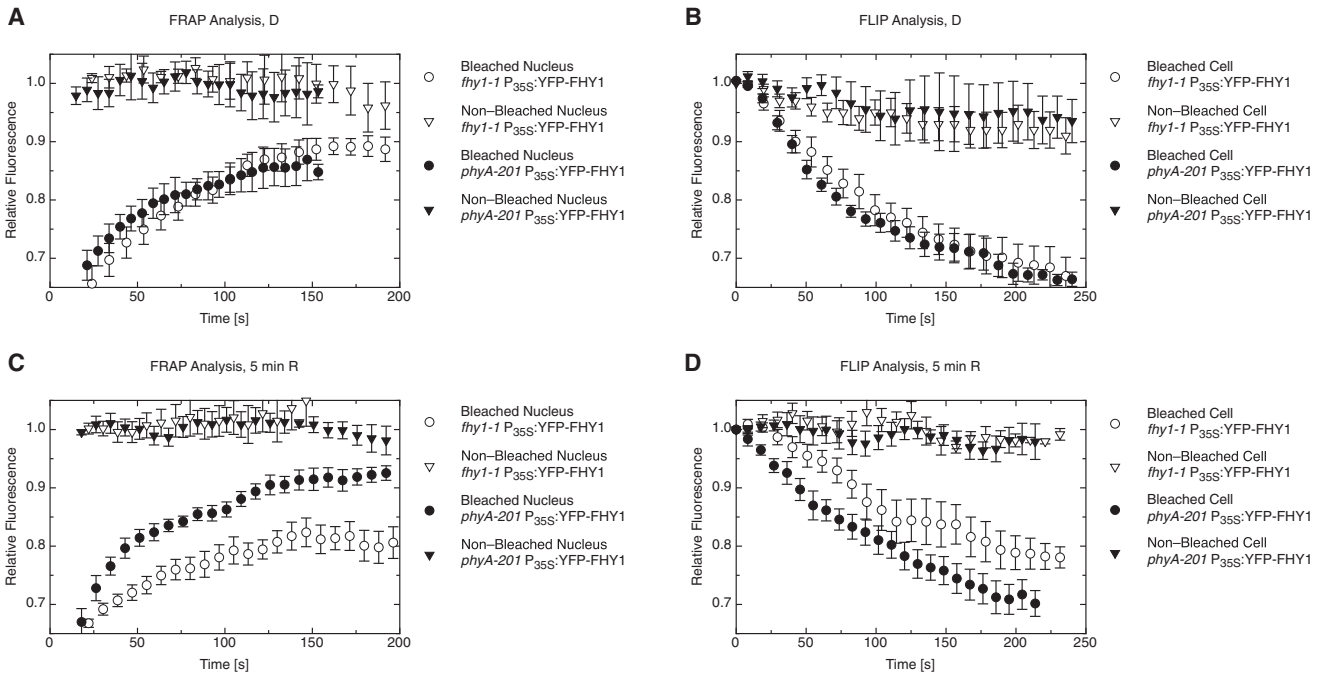

Figure 1. FHY1 Nucleocytoplasmic Shuttling

(A and B) FHY1 is mobile between the cytosol and the nucleus.

(A) For FRAP assays, 3-day-old etiolated *fhy1-1* (open symbols) and *phyA-201* seedlings (filled symbols) expressing P_{35S}:YFP-FHY1 (YFP-FHY1 under the control of the constitutive 35S promoter) were used. After bleaching the nucleus of a cell, the recovery of the fluorescence was recorded in the bleached nucleus (circles) and, as a control, in a neighboring nonbleached nucleus (triangles). n = 6. Error bars represent SEM.

(B) Seedlings for FLIP assays were grown as described in (A). While continuously bleaching an area in the cytosol of a cell, the loss of fluorescence in the nucleus of the same cell was recorded (circles). As a control, the fluorescence in the nucleus of a nonbleached cell was measured (triangles). n = 6. Error bars represent SEM.

(C and D) Interaction with phyA slows down shuttling of FHY1. (C) Three-day-old etiolated *fhy1-1* (open symbols) and *phyA-201* (filled symbols) seedlings expressing P_{35S}:YFP-FHY1 were irradiated for 5 min with R (15 μmol m^{-2} s^{-1}) and used for FRAP analyses as described in (A). n = 6. Error bars represent SEM.

(D) The seedlings were grown as in (C) and used for FLIP experiments as described in (B). n = 6. Error bars represent SEM.

PhyA Y242H Is Constitutively in the Pfr Form

PhyA Y242H is predicted to be constitutively in Pfr (Su and Lagarias, 2007). In yeast two-hybrid assays, binding of phyA to FHY1, FHL, PIF1, and PIF3 was dependent on light, i.e., on conditions establishing high levels of Pfr. In contrast, phyA Y242H did interact with FHY1, FHL, PIF1, and PIF3 in a light-independent manner, indicating that it is constitutively in Pfr or at least in a Pfr-like conformation (Figures 2A and 2B). Previously, it was shown that the phyA-FHY1/FHL complex rapidly dissociates when phyA is converted to Pr (Genoud et al., 2008; Sorokina et al., 2009). In contrast, in yeast two-hybrid assays, phyA Y242H-FHY1/FHL complexes were stable irrespective of the light conditions (Figure 2C). This further supports the notion that phyA Y242H is constitutively in Pfr and cannot be converted to Pr by any light treatment.

Su and Lagarias (2007) showed that phyB Y276H still depends on the chromophore for physiological activity. Consistent with this notion, we found that mutating cysteine 323 in phyA, which is essential for chromophore binding, to an alanine (C323A) abolished the interaction of phyA Y242H and FHY1 (Figure 2A).

Mathematical Model Exhibits Maximal Action in FR

Although phyA Y242H-YFP is constitutively in Pfr, it is virtually inactive at the physiological level, and seedlings expressing phyA Y242H-YFP exhibit only a weak *cop* phenotype (Figure 3A and Figure S3) (Su and Lagarias, 2007). Thus, not only Pr→Pfr but also Pfr→Pr conversion seems to be essential for proper phyA function. Based on these findings, we propose a model for light- and FHY1/FHL-dependent phyA nuclear transport, which consists of three overlapping cycles: two Pr/Pfr photoconversion cycles—one in the cytosol and one in the nucleus—and one FHY1/FHL-Pr/Pfr complex association/dissociation cycle, which links the two photoconversion cycles (Figure 4A and Figure S4A). In this model, FHY1/FHL continuously shuttle between the cytosol and the nucleus. They bind reversibly to phyA in the cytosol and transport it into the nucleus. After dissociation, FHY1/FHL are recycled back to the cytosol.

Due to the nonlinearity of the system shown in Figure 4A, which arises from the phyA-FHY1/FHL complex formation, the dynamics cannot be predicted without a more detailed mathematical analysis. As most of the biochemical parameters of the model depicted in Figure 4A are unknown and difficult to determine experimentally, a qualitative global network analysis was employed (Clodong et al., 2007; von Dassow et al., 2000). The emerging reaction scheme is described by a system of coupled ordinary differential equations (see Supplemental Information).

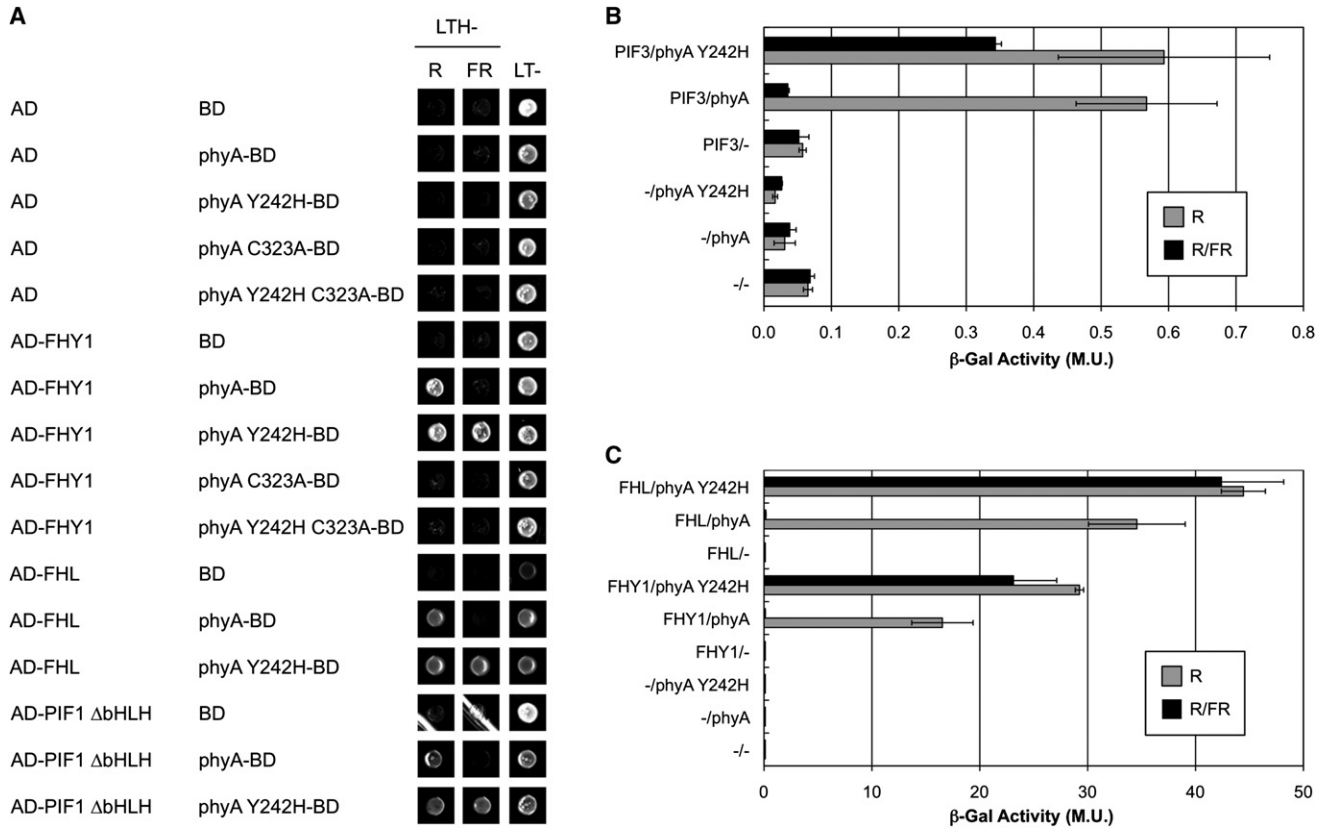

Figure 2. Constitutive Interaction of PhyA Y242H and FHY1/FHL

(A) PhyA Y242H constitutively interacts with FHY1, FHL, and PIF1. Yeast cells coexpressing the indicated plasmid constructs were grown on nonselective plates (CSM LT-) or on selective plates (CSM LTH-) supplemented with 1 mM 3-AT and 10 μM PCB (phycocyanobilin). The selective plates were incubated in FR (15 μmol m^{-2} s^{-1}) or R (1 μmol m^{-2} s^{-1}) to convert phyA to Pr and Pfr, respectively. AD, GAL4 activation domain; BD, GAL4 DNA-binding domain.

(B) PhyA Y242H constitutively interacts with PIF3. Yeast cells transformed with the indicated plasmids were used for an ONPG assay. The yeast cultures were irradiated for 5 min with R (15 μmol m^{-2} s^{-1}), either followed by a 5 min FR (15 μmol m^{-2} s^{-1}) treatment (R/FR) or not (R), and were incubated for another 4 hr before measuring the β-Gal activity. n = 3. Error bars represent SEM.

(C) PhyA Y242H cannot be converted to Pr. Yeast cells were transformed with the indicated plasmids and used for an ONPG assay as described in (B). n = 3. Error bars indicate SEM.

See also Figure S2.

To study the qualitative behavior of the rescaled dynamic reaction scheme of Figure 4A and Figure S4B, we defined a list of input conditions, including the observations that FHY1/FHL protein levels positively correlate with the action of phyA and that expression of phyA Y242H-YFP reduces the hypocotyl length in dark-grown seedlings but interferes with hypocotyl growth inhibition in FR (Figure 4B). Although the list of input conditions includes the requirement that the simulated action spectrum exhibits a peak, we did not restrict its position to a specific wavelength. As output, we used the amount of nuclear-localized Pfr (= Pfrn). A systematic scan of the parameter space (Table S1) found those combinations, which reproduced all of the input conditions, defining the "admissible parameter space" of the problem posed. Among 10^6 randomly chosen parameter sets, we found 6050 admissible parameter combinations (~1 in 165), for each of which we simulated an action spectrum between 640 and 720 nm. Surprisingly, almost all admissible combinations resulted in an action spectrum with a peak in FR (Figures 5A and 5B). Hence, the underlying structure of the dynamic model and the input conditions defined in Figure 4B result in an obligate shift of the action peak to FR as seen for the HIR (Hartmann, 1967; Shinomura et al., 2000; Dieterle et al., 2001) (Figure S1).

Efficient phyA nuclear accumulation requires continuous irradiation with FR despite maximal Pfr abundance in R, which reflects the distinctive features of the HIR (Kim et al., 2000). Thus, the crucial test for the theoretical description of the phyA dynamics is whether the model correctly predicts the nuclear abundance of phyA in R and FR. A simulation revealed that, for 92% of all admissible parameter combinations (total 5566, ~1 in 179), the total amount of phyA accumulating in the nucleus was higher at 720 nm than at 660 nm.

Sensitivity Analysis

To study the sensitivity to variations of individual parameters, we took the remaining 5566 admissible parameter combinations and varied one parameter value at a time while holding all of

the others fixed (see Supplemental Information). The position of the action peak was mainly influenced by the Pfr-FHY1 complex dissociation rate, followed by the Pfr degradation rate (Figure 5C). Decreasing the Pfr degradation rate shifted the position of maximal activity to shorter wavelengths (Figure S5A), whereas the shift of the peak due to variation of the Pfr-FHY1 complex dissociation rate is not uniform throughout the admissible parameter space (Figure S5B; see Supplemental Information). Varying the other parameters only weakly influenced the peak position. Considering the peak height, we found that the total amount of FHY1 and FHL (f_0), as well as the Pfr degradation rate, were the most crucial parameters affecting the amount of nuclear-localized Pfr (Figure 5D). Decreasing the Pfr degradation rate increased the peak height (Figure S5C). It has been shown that FHY1/FHL-overexpressing seedlings are hypersensitive to FR, whereas *fhy1* and *fhy1 fhl* mutant plants are hyposensitive (Desnos et al., 2001; Whitelam et al., 1993; Zhou et al., 2005). Variation of the parameter f_0 affected the peak height in a way that is consistent with these reports (Figure S5D). For all other parameters, we found a rather low sensitivity with respect to the height of the action peak. Note that the sensitivities of peak height and position are mostly nuclear specific (insets Figures 5C and 5D; see Supplemental Information).

Experimental Verification of Model Predictions

According to the model's predictions, inserting a nuclear localization signal (NLS) into phyA Y242H-YFP or increasing the FHY1 levels in phyA Y242H-YFP-expressing plants should result in completely light-independent signaling (Table S2; see Supplemental Information). To validate the predictive power of the model, we verified these key predictions experimentally by generating transgenic seedlings expressing phyA Y242H-NLS-YFP or phyA Y242H-YFP in the presence of 35S promoter-driven CFP-FHY1.

Although phyA Y242H-NLS-YFP was present at very low levels, it induced a strong *cop* phenotype in dark-grown Col-0 and *phyA* seedlings (Figure 6A). Moreover, FR-grown Col-0 seedlings expressing phyA Y242H-NLS-YFP were indistinguishable from the wild-type, suggesting that inserting a NLS into phyA Y242H-YFP is sufficient to suppress its dominant-negative effect. Overexpression of FHY1 in phyA Y242H-YFP-containing plants resulted in a strong *cop* phenotype as well (Figure 6D). In accordance with the idea that phyA Y242H-YFP interferes with FHY1 recycling, we found that increasing the FHY1 levels strongly promotes nuclear accumulation of phyA Y242H-YFP (Figure 6E).

To demonstrate that inserting a NLS into phyA Y242H-YFP specifically overcomes defects in nuclear transport, but not in downstream signaling, we crossed Col-0 P_{PHYA}:PHYA Y242H-NLS-YFP seedlings into the *hy5* mutant, which is defective in transduction of light signals (Oyama et al., 1997). Irrespective of whether grown in D (dark) or FR, *hy5* P_{PHYA}:PHYA Y242H-NLS-YFP seedlings had much longer hypocotyls than the parent line expressing the same construct in wild-type background (Figure 6B). Microscopy studies confirmed the nuclear localization of phyA Y242H-NLS-YFP in both Col-0 and *hy5* seedlings (Figure S6A).

When grown on medium supplemented with sucrose seedlings expressing phyA Y242H-NLS-YFP continued photomorphogenic growth in complete darkness, developed leaves, and started to flower after 6 weeks (Figure 6C and Figures S6B–S6D). Under these conditions, other photoreceptors (phyB-E, cryptochromes, phototropins, UV-B receptors) are inactive, suggesting that phyA is sufficient for the development from seeds to flowering plants.

Unraveling the Core Mechanisms for Shifting the Action Peak to FR

In the previous sections, we have shown that our model (Figure 4A) for the phyA dynamics is capable of reproducing the observed wavelength shift in the action spectrum and that this property prevails in most of the admissible parameter space defined by the input conditions given in Figure 4B. To identify the core mechanism being responsible for the wavelength shift, we adopted an abstract viewpoint on the phyA dynamics. We constructed networks using the key property of phytochromes—namely, their capability of interconversion between different states via light absorption. A generic network consists of vertexes, i.e., different states, and edges, i.e., transitions between the states. The edges can be light regulated—like the transition between Pr and Pfr—or light independent. Because we singled out a state as being the effector for further downstream signaling, we considered the direction from the influx into the network, i.e., synthesis, to the effector as being the forward direction. Therefore, we distinguished between two types of light-dependent edges. Type I consists of the light-induced transition from a state X to a different state Y at rate of the Pr→Pfr transition (k_1) and the back transition from Y to X with rate of the Pfr→Pr conversion (k_2). Type II represents the reversed edge, i.e., light-induced transition from X to Y at rate k_2 and the back transition from Y to X at rate k_1 (Figure 7A). This means that the forward directions of the edges exhibit the wavelength characteristics of the Pr form (type I) and the Pfr form (type II), with maxima at 667 nm and 730 nm, respectively. In addition, light-independent transitions between states (type 0 edges; e.g., biochemical reactions or transport events) could occur as well as synthesis and degradation at the vertexes. For simplicity, we considered synthesis or influx into the network only at one vertex, which is attached to a type I edge. This reflects that phytochromes are synthesized in the Pr state and activated by the light-induced transition to Pfr. Moreover, we considered the wavelength-dependent abundance of the effector as the action spectrum of the network.

The simplest network that one can construct with the elements summarized in Figure 7A is the network with influx into state X connected to Y by an edge of type I (Figure 7B). This represents the phytochrome reaction network in which X is the Pr and Y the Pfr form (Schäfer and Mohr, 1974). The corresponding action spectra given by the abundance of Y are shown in Figure 7B. For low fluence rates (see Supplemental Information), the action spectrum resembled the Pr absorption spectrum (Mancinelli, 1994), whereas it became virtually independent of the wavelength for high fluence rates, approaching the photo-equilibrium. The position of the maxima was almost independent of the parameters and coincided with the position of the Pr absorption maximum (Mancinelli, 1994), which was expected for this simple network. To obtain a network exhibiting maximal response in FR instead of R, we proceeded by adding an edge of type II, the

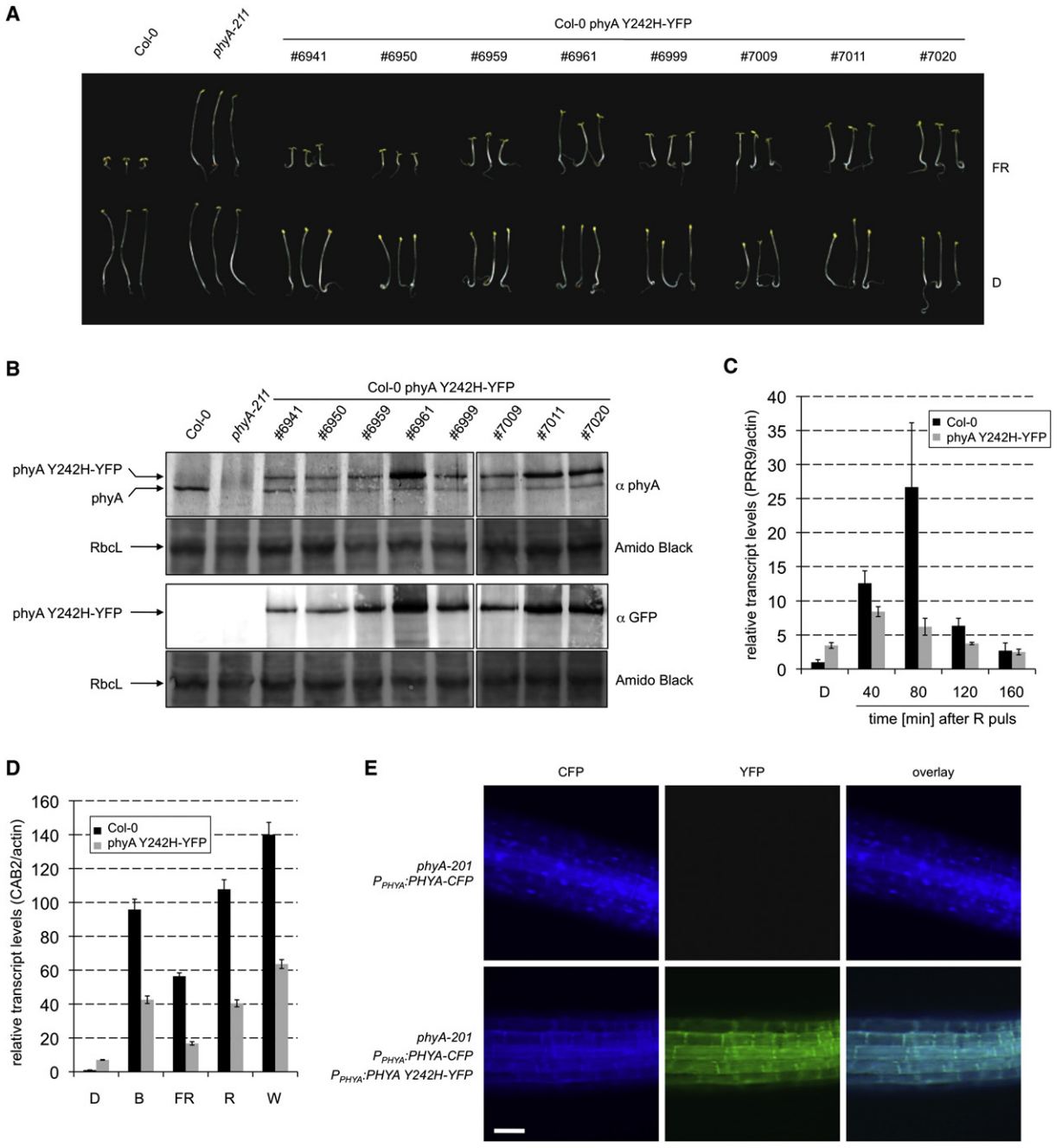

Figure 3. The PhyA Y242H-YFP Phenotype

(A) Expression of phyA Y242H-YFP interferes with FR perception. Wild-type (*Arabidopsis* Col-0), as well as several independent transgenic lines expressing P_{PHYA}:PHYA Y242H-YFP in Col-0 background, were grown for 4 days in D (dark) or FR (15 μmol m^{-2} s^{-1}).

(B) PhyA Y242H-YFP expression levels correlate with the strength of the phenotype. Fifteen μg of total protein isolated from 4-day-old dark-grown seedlings (Col-0, *phyA-211*, several independent lines expressing P_{PHYA}:PHYA Y242H-YFP in Col-0) were analyzed by immunoblotting with antibodies against phyA or GFP. A section of the amido black-stained membrane is shown as loading control.

(C) PRR9 transcript levels in phyA Y242H-YFP seedlings. Five-day-old, dark-grown Col-0 and Col-0 P_{PHYA}:PHYA Y242H-YFP (line #6941) seedlings were irradiated for 30 s with R (0.042 μmol m^{-2} s^{-1}) and were incubated for different time periods in D before RNA extraction. The transcript levels of PRR9 and ACTIN1 were determined by real-time RT-PCR. The expression levels of PRR9 were normalized to the levels of ACTIN1 (Col-0 in D was set to 1). Error bars represent SD.

(D) CAB2 transcript levels in phyA Y242H-YFP seedlings. Col-0 and Col-0 P_{PHYA}:PHYA Y242H-YFP (line #6941) seedlings were grown for 4 days in D and either irradiated for 24 hr with B, FR, R, or W or incubated for another 24 hr in D before RNA extraction. Real-time RT-PCR analyses were done as described in (C). The expression levels of CAB2 were normalized to the levels of ACTIN1 (Col-0 in D was set to 1). Error bars represent SD.

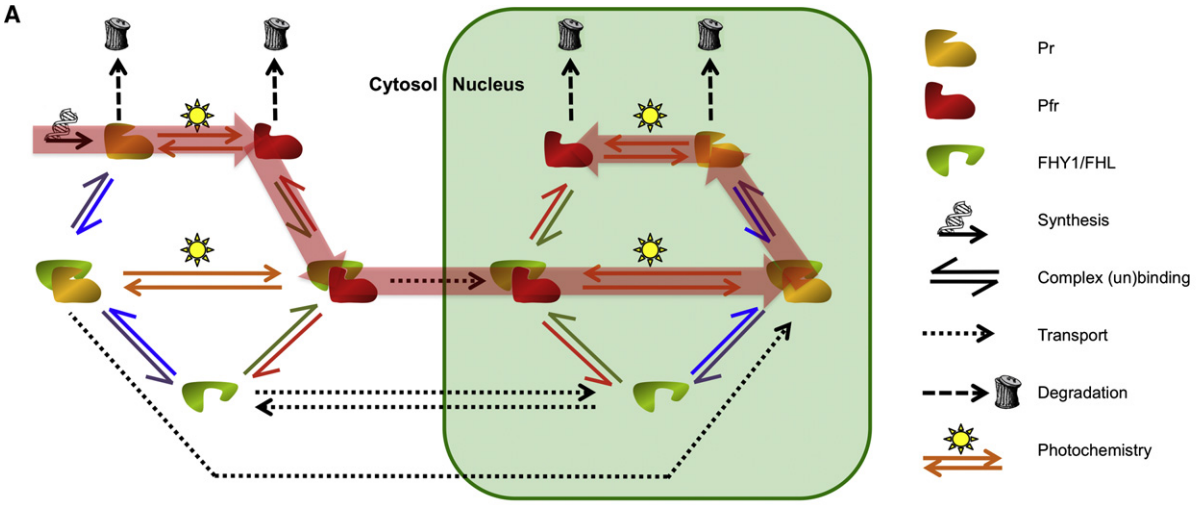

B

Input conditions

Condition	Experimental phentoype	Transfer to model	Reference
phyA-YFP in D	phyA-YFP localizes to the cytosol	$phy_{nuc} \leq 5\%$ in D	Hiltbrunner et al., 2005; Kim et al., 2000
phyA-YFP in cFR	phyA-YFP accumulates in the nucleus	$phy_{nuc} \geq 10\%$ in cFR	Hiltbrunner et al., 2005; Kim et al., 2000
phyA Y242H-YFP in D	Hypocotyls are shorter in phyA Y242H-YFP plants than in wt	Pfrn(wt) < Pfrn(phyA Y242H-YFP) in D	Fig. S3
phyA Y242H-YFP in cFR	Hypocotyls are longer in phyA Y242H-YFP plants than in wt	Pfrn(wt) > Pfrn(phyA Y242H-YFP) in cFR	Fig. S3
fhy1 in cFR	Hypocotyls are longer in *fhy1* than in wt	Pfrn(wt) > Pfrn(*fhy1*) in cFR	Desnos et al., 2001; Whitelam et al., 1993; Zeidler et al., 2001
FHY1 OX in cFR	Hypocotyls are shorter in FHY1 OX lines than in wt	Pfrn(wt) < Pfrn(FHY1 OX) in cFR	Desnos et al., 2001
Varying wavelength λ	wt exhibits peak in action spectrum (any position)	Calculate Pfrn(wt) for different λ; find peak: $Pfrn(wt(\lambda_{max} \pm 20\ nm)) \leq 0.9 \times Pfrn(wt(\lambda_{max}))$	

Figure 4. PhyA Signaling Model and Input Conditions for the Parameter Scan

(A) Dynamic model for phyA nuclear transport. See Figure S4B for parameter names. The HIR module (see text) is labeled in red.

(B) Experimental input conditions used for parameter scan. phy_{nuc}, nuclear-localized phytochrome (refer to Figure S5 for exact definition). cFR, continuous FR. See also Figure S4, Figure S5, and Table S1.

reversed light-dependent edge. For low fluence rates, the maximal response of the extended network is close to the Pr absorption maximum (which is reminiscent of the VLFR), whereas it is strongly shifted toward FR for high fluence rates (Figure 7C and Figure S7). Therefore, we discovered the smallest network (hereafter referred to as "HIR module" or "shifting module") with an absorption maximum in R but exhibiting maximal response in FR under high irradiance conditions. Note that synthesis and degradation are absolutely essential ingredients that result in a constant particle flux through the network and render the system out of equilibrium. Thus, all explanations for the HIR based on equilibrium considerations are doomed to fail. The other essential ingredients, in addition to synthesis and degradation, are the type I and type II edges, which have to occur pairwise in the pathway from the influx to the effector. They do not have to be linked directly to each other and may be separated by one or several type 0 edges. For an extended analysis and discussion, see the Supplemental Information.

There is a simple way to understand why the pair of type I/type II edges produces a shift in the action spectrum. The transition from Pfr→Pr has its maximum in FR (Mancinelli, 1994), and hence it is essential to have a type II edge in forward direction, i.e., from synthesis to the signaling state. However, as phyA is synthesized in the Pr form, it first needs to be converted to Pfr, which requires a type I edge in forward direction. To have both transitions in forward direction in the pathway, it is indispensable that the initial Pr form and the final Pr form are different, i.e., Pr→Pfr→Pr*. How this can be achieved in planta is discussed in the

(E) PhyA Y242H-YFP inhibits nuclear accumulation of wild-type phyA. *PhyA-201* P_{PHYA}:PHYA Y242H-YFP was crossed into *phyA-201* P_{PHYA}:PHYA-CFP background. In the F2 generation, individuals homozygous for both transgenes were selected. Four-day-old dark-grown *phyA-201* P_{PHYA}:PHYA-CFP and *phyA-201* P_{PHYA}:PHYA-CFP P_{PHYA}:PHYA Y242H-YFP seedlings were irradiated with FR (15 μmol m^{-2} s^{-1}) for 6 hr and were used for microscopy. Scale bar, 100 μm.

See also Figure S3.

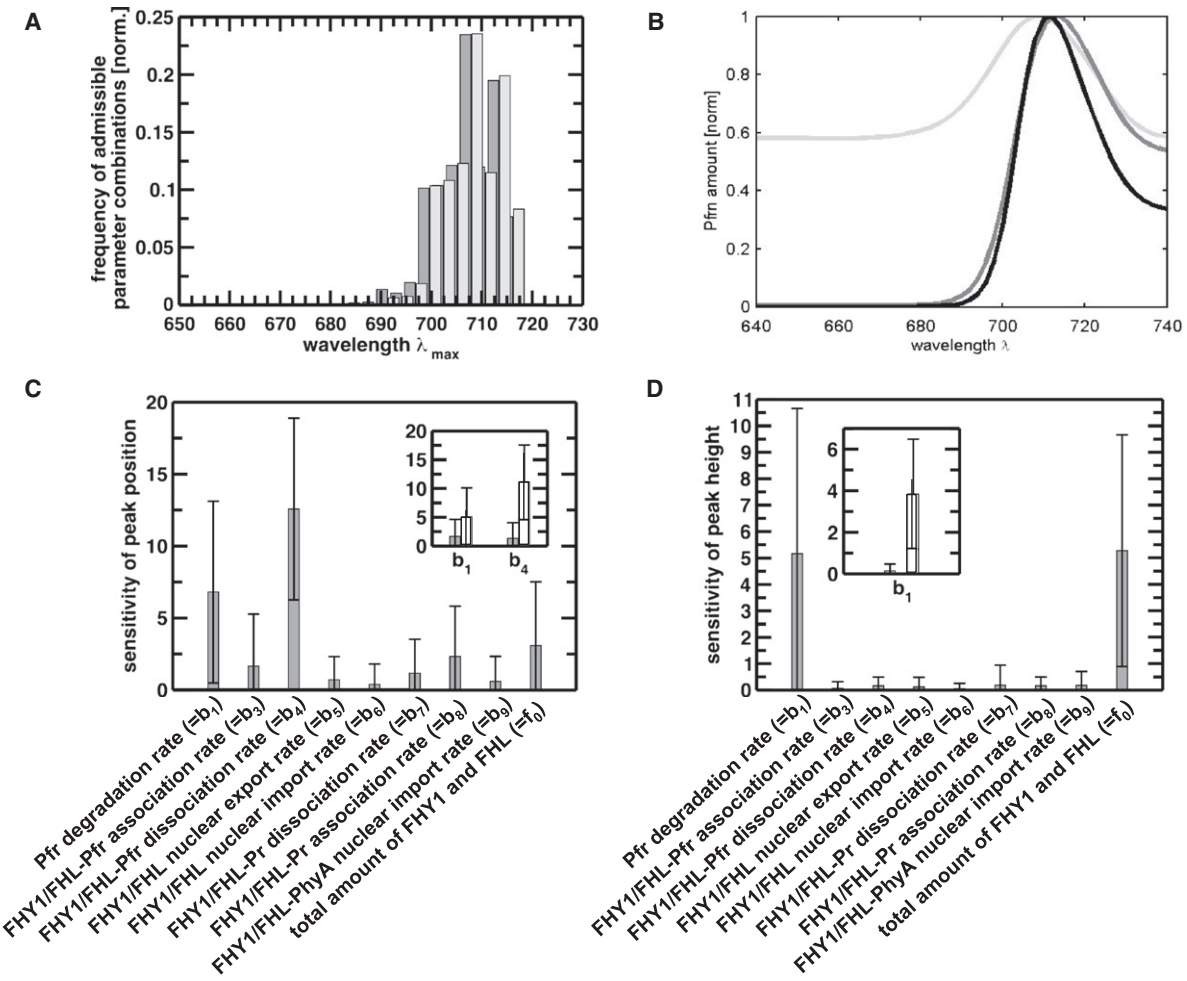

Figure 5. Simulation Results

(A) Distributions of the admissible parameter combinations exhibiting maximal action at wavelength λ_{max} when assuming the input conditions of Figure 4B (dark gray) or additionally assuming $phy_{nuc}(660nm) < phy_{nuc}(720nm)$ (light gray). The distributions were normalized to the total number of admissible parameters.

(B) Representative action spectra (for three arbitrary admissible parameter combinations) based on the relative and saturated amount of Pfrn in FR irradiation.

(C and D) Parameter sensitivity of the dynamic constants with respect to the peak position (C) and the peak height (D). The insets show the contributions from the cytosolic (gray) and the nuclear (white) parameter variations. Error bars represent SD.

See also Figure S5 and Figure S7.

next section. Whether the wavelength characteristic of the Pr→Pfr transition (peak at 667 nm) or the Pfr→Pr transition (peak at 730 nm) dominates depends on the degradation rates and the light intensity (see Supplemental Information). It is important to note that, in order to obtain the shift of the action peak from R to FR, the degradation rate of the intermediate state (Y in Figure 7C) needs to be higher than that of the initial state (X in Figure 7C; see Supplemental Information). Thus, it follows that, in a realistic phyA network, the stability of the intermediate Pfr state has to be reduced compared to the stability of the Pr state, which is in accordance with experimental data (Hennig et al., 2000).

To investigate the effect of having more than one HIR module, we concatenated several modules, with influx into the first module and state Z of the last module being the effector (Figure 7D). The serial connection of wavelength-shifting modules resulted in sharpening of the peak, which, in planta, may be important to better separate the action of phyA from that of other phytochromes (e.g., phyB) having an action peak in R. Using measured data (Dieterle et al., 2001), we estimated that the shift and the observed narrow range of the phyA action spectrum in planta is achieved by concatenating three to four shifting modules (see Supplemental Information).

Network Realization In Planta

Using an abstract viewpoint, we unraveled the essential building elements to construct a network with an absorption maximum in R but maximal response in FR. In Figures 7E–7G, we suggest three different possibilities of how such a network can be realized *in planta*. The first one is that, upon binding to a kinase, phyA is phosphorylated (Figure 7E). It is important that the kinase dominantly and strongly binds to Pfr. This ensures that the reversed light-induced transformation is indispensable to release

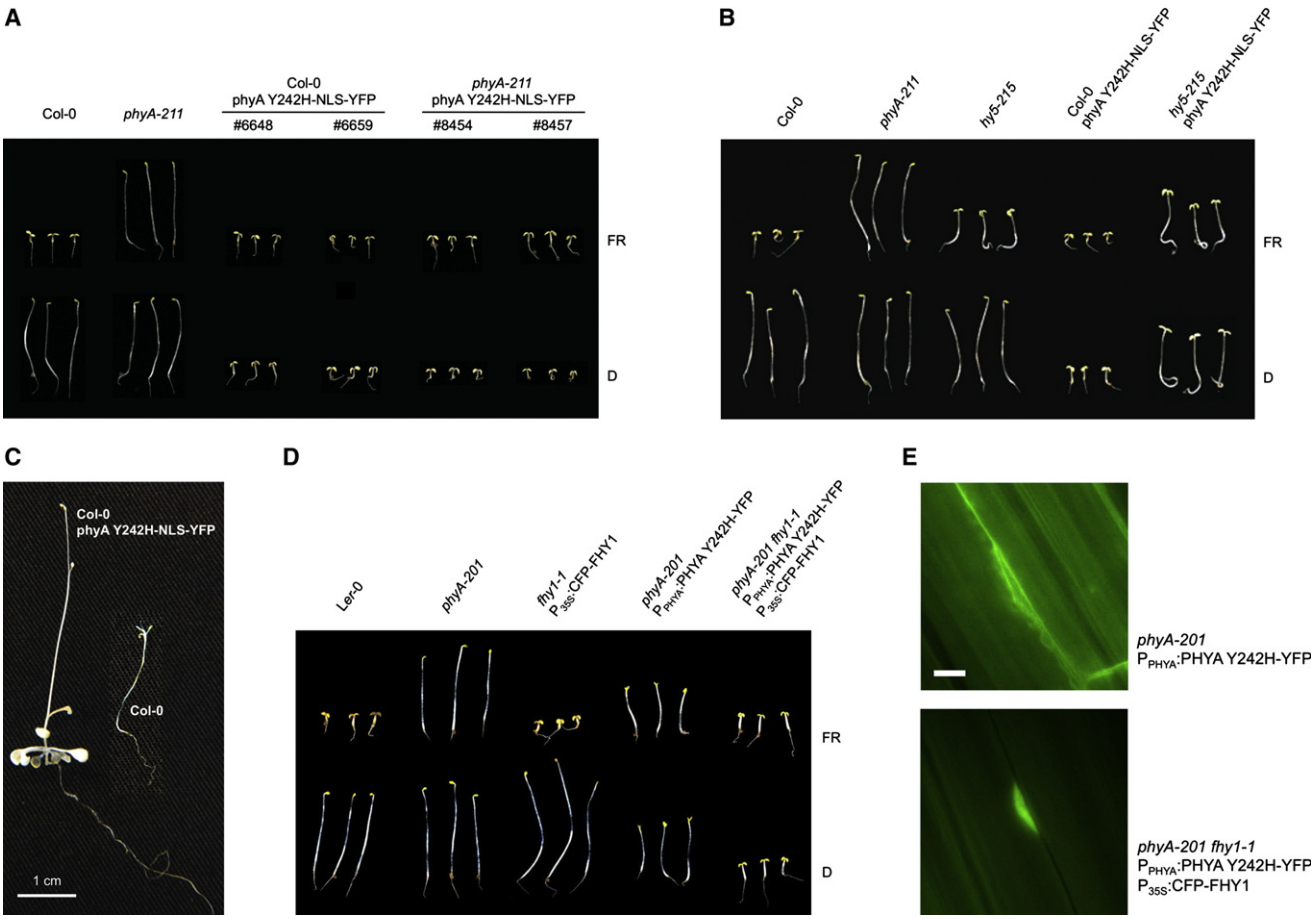

Figure 6. PhyA Y242H-NLS-YFP Seedlings Exhibit a *cop* Phenotype

(A) Targeting phyA Y242H-YFP to the nucleus results in a *cop* phenotype. Wild-type (*Arabidopsis* Col-0) and *phyA-211* seedlings, as well as independent transgenic lines expressing P_{PHYA}:PHYA Y242H-NLS-YFP in Col-0 or *phyA-211* background, were grown for 4 days in D or FR (15 μmol m^{-2} s^{-1}).

(B) The *hy5* mutant reduces the *cop* phenotype of phyA Y242H-NLS-YFP-expressing lines. Col-0 P_{PHYA}:PHYA Y242H-NLS-YFP (line #6648) was crossed into *hy5-215* mutant background. Col-0, *phyA-211*, and *hy5-215* seedlings, as well as transgenic lines expressing P_{PHYA}:PHYA Y242H-NLS-YFP in Col-0 or *hy5-215* background, were grown for 4 days in D or FR (15 μmol m^{-2} s^{-1}).

(C) PhyA Y242H-NLS-YFP-expressing plants flower in D. Col-0 plants expressing P_{PHYA}:PHYA Y242H-NLS-YFP were grown for 6 weeks in the dark on 1/2 × MS, 0.7% agar supplemented with 1% sucrose.

(D) Overexpression of FHY1 induces a strong *cop* phenotype in phyA Y242H-YFP seedlings. *PhyA-201* seedlings expressing P_{PHYA}:PHYA Y242H-YFP were crossed into *fhy1-1* P_{35S}:CFP-FHY1 background. A line that is homozygous for the *phyA-201* and *fhy1-1* mutations, as well as for both transgenes, was selected and grown for 4 days in D or FR (15 μmol m^{-2} s^{-1}). The respective parent lines, as well as wild-type (*Arabidopsis* Ler-0), *phyA-201*, and *fhy1-1* seedlings, were grown under the same conditions.

(E) PhyA Y242H-YFP accumulates in the nucleus of FHY1-overexpressing lines. *PhyA-201* P_{PHYA}:PHYA Y242H-YFP and *phyA-201 fhy1-1* P_{PHYA}:PHYA-YFP P_{35S}:CFP-FHY1 seedlings were grown for 4 days in D and were used for microscopic analysis. Only the YFP channel is shown. Scale bar, 5 μm.

See also Figure S6.

phosphorylated phyA, which is considered to be the effector. Alternatively, phyA interacts with another protein (C), which is subsequently marked (Figure 7F). The marked form of this protein is the active form for further downstream signaling. Again, it is important that the interacting protein C dominantly binds to Pfr. Finally, the network with the pair of type I/type II edges can also be realized using different compartments (Figure 7G). Here, Pfr strongly binds to a transport protein and is released after the light-induced back transformation to Pr. Note that, in all three examples, the Pfr complex dissociation rate needs to be significantly lower than k_2, the rate of Pfr→Pr photoconversion, and the stability of the Pfr complex must be higher than that of the Pr complex. Otherwise the type II edge, i.e., the light-induced conversion of Pfr→Pr, would not be necessary, and the HIR module would be lost.

The network presented in Figure 4A predominantly produces action spectra with peaks shifted toward FR. Comparing the signaling network shown in Figure 4A with the shifting modules presented in Figures 7E–7G reveals that, in the phyA-signaling network, the shifting module is realized using different compartments (Figures 7G and 7H; highlighted in Figure 4A). Thus, in planta, the pair of type I/type II edges is represented by the

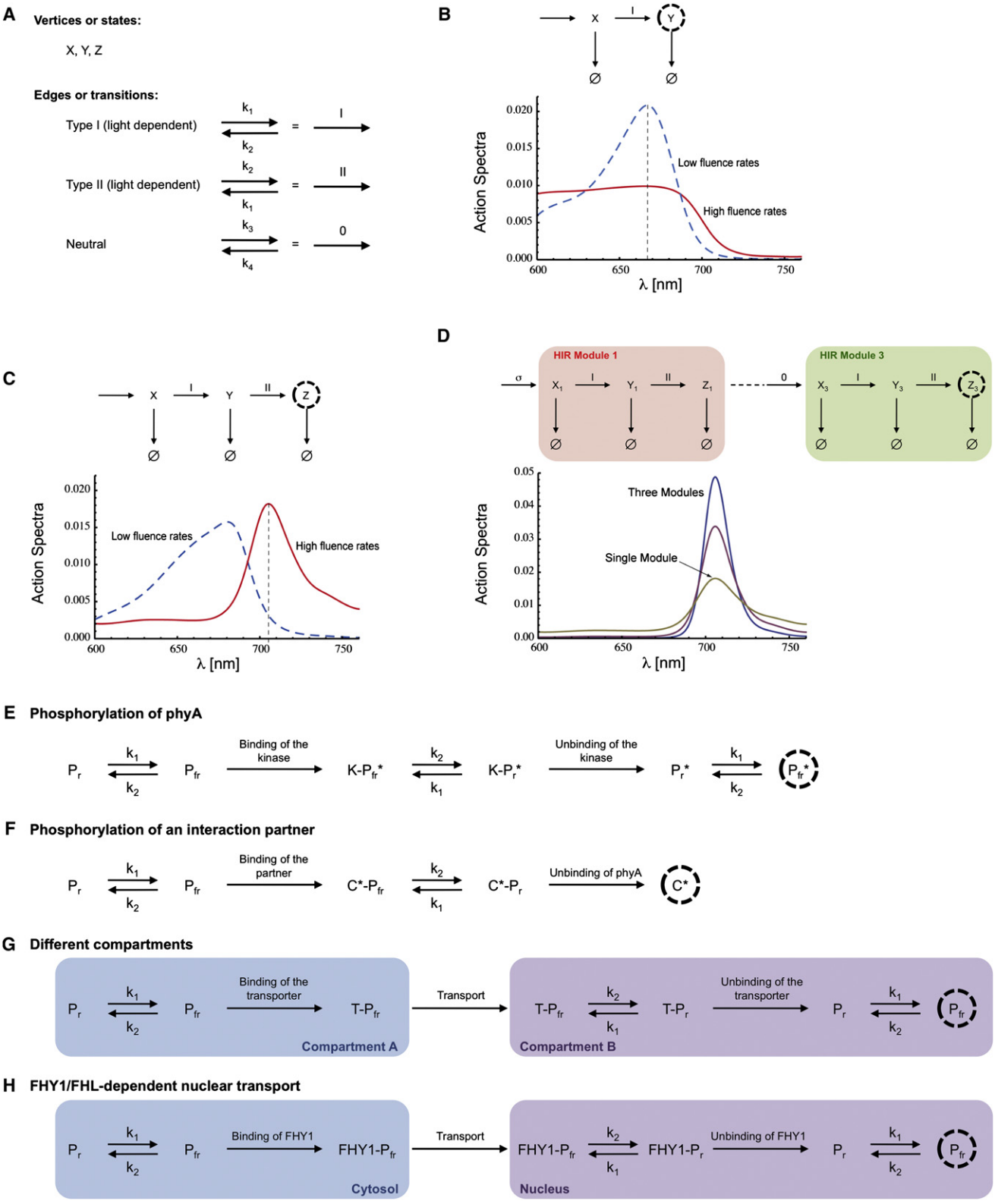

Figure 7. The Shifting Module

(A–D) Constructing a simple wavelength-shifting network.

(A) Basic construction elements.

cytosolic and nuclear photoconversion cycles, which operate in opposite directions. As both photoconversion cycles are essential to generate the shift of the action peak from R to FR, the FHY1-Pfr complex dissociation rate needs to be lower than the rate of Pfr→Pr photoconversion, and the FHY1-Pfr complex has to be more stable than the FHY1-Pr complex. Consistent with these requirements, yeast two-hybrid and in vitro pull-down assays support the idea that FHY1-Pfr complexes are more stable than FHY1-Pr complexes (Hiltbrunner et al., 2005, 2006; Sorokina et al., 2009). However, despite the fact that the Pfr/Ptot ratio is roughly 40-fold higher in R than FR, the amount of FHY1-phyA complexes in planta is higher in FR than in R, i.e., under conditions in which the Pfr/Ptot ratio is very low (Shen et al., 2009; Yang et al., 2009). Yet, our model is in agreement with this counterintuitive result. When we analyzed the relative levels of FHY1-phyA complexes, we found that, for 79% of the admissible parameters, the relative amount of FHY1-phyA complexes is higher at 726 nm (FR) than at 660 nm (R) (Figure S7C).

DISCUSSION

Three Cycles to Explain phyA Nuclear Accumulation

The core structure of our model for light- and FHY1/FHL-dependent phyA nuclear transport consists of a cytosolic and a nuclear-localized Pr/Pfr photoconversion cycle and an FHY1/FHL-Pr/Pfr complex association/dissociation cycle, which links the two photoconversion cycles (Figure S4 and Figure 4A). In this report, we suggest that photocycling between Pr and Pfr per se is essential for responsiveness to FR. Consistent with this notion, phyA mutant versions, which are constitutively in Pfr- or Pr-like states (i.e., phyA Y242H and phyA C323A), cannot substitute for wild-type phyA, which continuously cycles between Pr and Pfr when irradiated with light. It was shown that phyA-FHY1/FHL complexes rapidly dissociate after conversion of Pfr to Pr (Genoud et al., 2008; Sorokina et al., 2009). Thus, photocycling between Pr and Pfr results in continuous assembly and disassembly of phyA-FHY1/FHL complexes. Successive cycles of binding to FHY1/FHL in the cytosol and dissociation of phyA-FHY1/FHL transport complexes in the nucleus after photoconversion of Pfr to Pr would lead to nuclear accumulation of phyA. One concern with this model is that the half-life of Pfr-FHY1/FHL complexes may not be long enough to complete transport through the nuclear pore before photoconversion of Pfr to Pr results in dissociation of the complexes. However, active transport of NLS-containing proteins or protein complexes across the nuclear membrane requires 10–20 ms, whereas even in high fluence rate FR, the half-life of Pfr is roughly three orders of magnitude longer (Frey and Görlich, 2007; Mancinelli, 1994). Importantly, this model also offers an explanation for the fluence rate dependence of phyA nuclear transport. The rate of photocycling is proportional to the fluence rate, i.e., light intensity (Mancinelli, 1994). Thus, high light intensities (at least in the range occurring under natural conditions) would increase the transport capacity by increasing the rate of FHY1/FHL-phyA complex assembly and disassembly.

Toward Understanding the HIR in Molecular and Mathematical Terms

Although the Pfr/Ptot ratio is highest in R, phyA-mediated responses are most efficiently triggered by FR, in which the Pfr/tot ratio is roughly 40-fold lower than in R. PhyA is unique to higher plants and enables them to de-etiolate in shady habitats, which are characterized by a high FR content. As such, phyA may have provided an adaptive advantage to angiosperms, promoting their rapid radiation in the mid-Cretaceous (Mathews, 2005). The shift from maximal absorption in R to maximal activity in FR (Figure S1) has been known for more than half of a century (Mohr, 1957) but could not be linked to defined components or molecular events so far.

The mathematical model presented here integrates the current knowledge on phyA nuclear transport and degradation into a dynamic interaction network. A systematic sampling of the parameter space found the admissible parameter combinations for which the model in Figure 4A reproduced a list of input conditions, including the existence of a peak in the action spectrum. Although the position of the peak was not defined in the list of input conditions, the simulated action spectra exhibited a peak in FR throughout the admissible parameter space (Figure 5). Moreover, for almost all admissible parameter combinations, the total amount of phyA in the nucleus was maximal in FR. Therefore, the shift of the peak in the action spectrum from R to FR, as well as maximal nuclear accumulation of phyA in FR, are intrinsic features of our model (Figure 4A and Figure S4).

Defining the "HIR Module"

Our investigation of small light-regulated networks revealed the fundamental structural requirements for the HIR: nonequilibrium, i.e., synthesis and degradation, and a pair of reversed light-dependent edges in the pathway from synthesis to the effector.

Consistent with the scenario in Figure 7G, our model for phyA nuclear transport contains a pair of spatially separated, reversed light-dependent edges, i.e., the cytosolic and nuclear Pr/Pfr photoconversion cycles, which operate in opposite directions (Figure 4A, Figure 7H, and Figure S4). As both cycles are required to generate the shift of maximal action from R to FR, the

(B) Network reflecting the usual phytochrome reaction network.
(C) Response shifting/HIR module. The position of the action peak is fluence rate dependent and for high fluence rates in the FR region of the spectrum.
(D) Serial connection of several HIR modules. Concatenating multiple HIR modules leads to sharpening of the action peak.
(E–H) Possible network realization in planta.
(E) Binding of a kinase results in a phosphorylated phyA, which is the effector.
(F) Phosphorylation of a binding partner, which is the effector.
(G) Binding of a transporter, which transports phyA into a different compartment, where it acts as the effector.
(H) HIR module realized in planta.
See also Figure S7.

FHY1-Pfr complex dissociation rate has to be lower than k_2, the rate of Pfr→Pr photoconversion, and the stability of the Pfr-FHY1 complex needs to be higher than that of the Pr-FHY1 complex. Bypassing the need of the Pfr→Pr photoconversion cycle in the nucleus by having an FHY1-Pfr complex dissociation rate higher than k_2 and/or a lower stability of the Pfr-FHY1 than the Pr-FHY1 complex would result in a loss of the HIR module.

Importantly, our analysis also revealed that phyA degradation is essential not only to prevent excessive signaling and interference with the shade avoidance response (Debrieux and Fankhauser, 2010), but also to obtain a maximal response in FR.

"Ecological" Relevance and Evolution of the HIR

PhyA is the most abundant phytochrome species in etiolated seedlings, whereas phyB dominates in plants grown in light. It has been hypothesized that degradation of phyA in R is important to clearly separate between the action of phyA and phyB. An alternative way to increase the specificity between phyA and phyB is to sharpen the peaks of their action spectra in order to minimize the overlap. For phyA, this can be achieved by concatenating several HIR modules, as shown in Figure 7D. Based on our theoretical analysis, we estimate the number of HIR modules in planta to be three to four. So far, we discovered one of these modules, the FHY1 import cycle. It is well established that phyA nuclear transport is a prerequisite for FR perception and that it works most efficiently under HIR conditions (Hiltbrunner et al., 2006; Kim et al., 2000; Rösler et al., 2007). These findings are consistent with the idea that the FHY1 import cycle is one of the HIR modules. In line with our estimate, there is strong experimental evidence for the existence of additional HIR modules. Fusing a NLS directly to phyA bypasses the FHY1 import cycle (i.e., the "first" HIR module) and, as a consequence, should result in a loss of the R→FR shift of the action peak. Yet, phyA localizing constitutively to the nucleus perfectly responds to FR, and expression of phyA-NLS restores sensitivity to FR in the absence of FHY1 (Genoud et al., 2008). This strongly argues for the existence of at least one additional HIR module acting in the nucleus (i.e., downstream of phyA nuclear transport).

Light filtering through the foliage of forest trees is depleted of photosynthetically active radiation (mainly B and R) and is strongly enriched in FR. The colonization of understory areas has been associated with the emergence of a photoreceptor system that is able to perceive FR (Mathews, 2005). Data presented in this report suggest that higher plants acquired such a FR sensing system by using a photoreceptor with maximal absorption in R and adjusting its molecular interactions rather than changing the photophysical properties of the photoreceptor itself. The Pr and Pfr absorption spectra of phyA and phyB are virtually identical, whereas the action spectra differ dramatically, with phyA having an action peak in FR and phyB in R (Eichenberg et al., 2000; Hartmann, 1967; Shinomura et al., 1996, 2000). Two main differences between phyA and phyB are the Pfr degradation rate and the mechanism employed for nuclear transport. Whereas phyA is rapidly degraded in Pfr, phyB is much more stable and, in contrast to phyA, does not depend on FHY1/FHL for nuclear transport (Bae and Choi, 2008; Hiltbrunner et al., 2006). Strong Pfr degradation and the FHY1/FHL transport cycle are essential components of the HIR module that we identified. Increasing the Pfr degradation rate of phyB and rendering its nuclear transport FHY1/FHL dependent may therefore result in a shift of its action peak toward FR. Currently, the amino acid residues that are responsible for the different behavior of phyA and phyB regarding Pfr stability and nuclear transport are unknown. However, once these residues have been identified, it seems feasible to recapitulate the evolution of the phyA-based FR sensing system that is present in today's plants by changing the respective residues in phyB and shifting its action peak to FR.

Conclusion

Previous models for the HIR assumed that neither dark-synthesized Pr nor photoconverted Pfr is the phyA species mediating the HIR but that it has to be modified in some way (Schäfer et al., 1975; Shinomura et al., 2000). Data presented in this report suggest that nuclear-localized Pfr is active in signaling (Figure 6) but that photocycling between Pr and Pfr is essential to shift the peak in the action spectrum from R to FR. This is consistent with the idea by Shinomura et al. (2000) that the HIR depends on photocycling of phyA. However, the strength of our model is that it provides an explanation in molecular and mathematical terms of why photocycling is essential for phyA nuclear transport and HIR signaling.

EXPERIMENTAL PROCEDURES

Fluorescence Microscopy and FRAP/FLIP Analyses

Fluorescence microscopy was done as described (Hiltbrunner et al., 2006). Three-day-old etiolated seedlings expressing P_{35S}:YFP-FHY1 in either *fhy1-1* or *phyA-201* background were used to perform FRAP and FLIP assays as described in the Extended Experimental Procedures.

Plasmid Constructs and Plant Material

A detailed description of the plasmid construct used in this study can be found in the Extended Experimental Procedures. The *phyA-201* (= *fre1-1*) and *fhy1-1* mutants (in L*er*), as well as the *phyA-211*, *fhy1-3* (= *pat3*), *fhl-1*, and *hy5-215* mutants (in Col) have been described (Desnos et al., 2001; Oyama et al., 1997; Quail et al., 1994; Whitelam et al., 1993; Zeidler et al., 2001; Zhou et al., 2005). Col-0 and L*er*-0 were used as wild-type.

The *fhy1-3 fhl-1* double mutant was obtained by crossing the respective single mutants. The transgenic lines expressing P_{35S}:YFP-FHY1 (*fhy1-1* pCHF70-FHY1) and P_{PHYA}:PHYA-CFP (*phyA-201* pphyA40-phyA) have been described (Genoud et al., 2008; Hiltbrunner et al., 2005). All other lines were obtained by Agrobacterium-mediated transformation or by crossing pre-existing lines, as described in the Extended Experimental Procedures. For details regarding growth conditions, refer to the Extended Experimental Procedures.

Yeast Two-Hybrid Assays, Immunoblot Analyses, and qPCR

Yeast two-hybrid growth and ONPG assays and immunoblot analyses were done as described (Genoud et al., 2008; Hiltbrunner et al., 2006). The antibody against phyA has been described in Hiltbrunner et al. (2006). Antibodies specific for green fluorescent protein (GFP)/YFP/CFP were purchased from Covance (Princeton, NJ, USA). qPCR was done according to standard protocols using gene-specific primers and probes for PRR9, CAB2, and ACTIN1. See the Extended Experimental Procedures for details.

SUPPLEMENTAL INFORMATION

Supplemental Information includes Extended Experimental Procedures, seven figures, and three tables and can be found with this article online at doi:10.1016/j.cell.2011.07.023.

ACKNOWLEDGMENTS

We are grateful to Dr. M. Zeidler and the ABRC for providing *fhy1-3* and *fhl-1* seeds. We thank Prof. J. Paszkowski for the kind gift of the pWCO35 plasmid, Dr. S. Kircher for support for FRAP/FLIP analyses, M. Krenz and C. König for technical assistance, and Prof. C. Fankhauser and Prof. R. Ulm for critically reading the manuscript. This work was supported by grants from the DFG to E.S. (SFB592) and to E.S. and J.T. (GRK1305, EXC294) and the BMBF-Freiburg Initiative in Systems Biology 0313921 (FRISYS) to C.F., J.T., and E.S.

Received: April 5, 2011
Revised: June 10, 2011
Accepted: July 13, 2011
Published: September 1, 2011

REFERENCES

Bae, G., and Choi, G. (2008). Decoding of light signals by plant phytochromes and their interacting proteins. Annu. Rev. Plant Biol. *59*, 281–311.

Casal, J.J., Luccioni, L.G., Oliverio, K.A., and Boccalandro, H.E. (2003). Light, phytochrome signalling and photomorphogenesis in *Arabidopsis*. Photochem. Photobiol. Sci. *2*, 625–636.

Clodong, S., Dühring, U., Kronk, L., Wilde, A., Axmann, I., Herzel, H., and Kollmann, M. (2007). Functioning and robustness of a bacterial circadian clock. Mol. Syst. Biol. *3*, 90.

Debrieux, D., and Fankhauser, C. (2010). Light-induced degradation of phyA is promoted by transfer of the photoreceptor into the nucleus. Plant Mol. Biol. *73*, 687–695.

Desnos, T., Puente, P., Whitelam, G.C., and Harberd, N.P. (2001). FHY1: a phytochrome A-specific signal transducer. Genes Dev. *15*, 2980–2990.

Devlin, P.F., Christie, J.M., and Terry, M.J. (2007). Many hands make light work. J. Exp. Bot. *58*, 3071–3077.

Dieterle, M., Zhou, Y.C., Schäfer, E., Funk, M., and Kretsch, T. (2001). EID1, an F-box protein involved in phytochrome A-specific light signaling. Genes Dev. *15*, 939–944.

Eichenberg, K., Bäurle, I., Paulo, N., Sharrock, R.A., Rüdiger, W., and Schäfer, E. (2000). *Arabidopsis* phytochromes C and E have different spectral characteristics from those of phytochromes A and B. FEBS Lett. *470*, 107–112.

Frey, S., and Görlich, D. (2007). A saturated FG-repeat hydrogel can reproduce the permeability properties of nuclear pore complexes. Cell *130*, 512–523.

Genoud, T., Schweizer, F., Tscheuschler, A., Debrieux, D., Casal, J.J., Schäfer, E., Hiltbrunner, A., and Fankhauser, C. (2008). FHY1 mediates nuclear import of the light-activated phytochrome A photoreceptor. PLoS Genet. *4*, e1000143.

Hartmann, K.M. (1967). [An action spectrum of photomorphogenesis under high energy conditions and its interpretation on the basis of phytochrome (hypocotyl growth inhibition in Lactuca sativa L)]. Z. Naturforsch. B *22*, 1172–1175.

Hennig, L., Büche, C., Eichenberg, K., and Schäfer, E. (1999). Dynamic properties of endogenous phytochrome A in *Arabidopsis* seedlings. Plant Physiol. *121*, 571–577.

Hennig, L., Büche, C., and Schäfer, E. (2000). Degradation of phytochrome A and the high irradiance response in *Arabidopsis*: a kinetic analysis. Plant Cell Environ. *23*, 727–734.

Hiltbrunner, A., Tscheuschler, A., Viczián, A., Kunkel, T., Kircher, S., and Schäfer, E. (2006). FHY1 and FHL act together to mediate nuclear accumulation of the phytochrome A photoreceptor. Plant Cell Physiol. *47*, 1023–1034.

Hiltbrunner, A., Viczián, A., Bury, E., Tscheuschler, A., Kircher, S., Tóth, R., Honsberger, A., Nagy, F., Fankhauser, C., and Schäfer, E. (2005). Nuclear accumulation of the phytochrome A photoreceptor requires FHY1. Curr. Biol. *15*, 2125–2130.

Hu, W., Su, Y.-S., and Lagarias, J.C. (2009). A light-independent allele of phytochrome B faithfully recapitulates photomorphogenic transcriptional networks. Mol. Plant *2*, 166–182.

Kim, L., Kircher, S., Toth, R., Adam, E., Schäfer, E., and Nagy, F. (2000). Light-induced nuclear import of phytochrome-A:GFP fusion proteins is differentially regulated in transgenic tobacco and *Arabidopsis*. Plant J. *22*, 125–133.

Mancinelli, A.L. (1994). The physiology of phytochrome action. In Photomorphogenesis in Plants, R.E. Kendrick and G.M.H. Kronenberg, eds. (Dordrecht: Kluwer Academic Publishers), pp. 211–269.

Mathews, S. (2005). Phytochrome evolution in green and nongreen plants. J. Hered. *96*, 197–204.

Mohr, H. (1957). Der Einfluss monochromatischer Strahlung auf das Längenwachstum des Hypocotyls und auf die Anthocyanbildung bei Keimlingen von *Sinapis alba* L. (=*Brassica alba* Boiss.). Planta *49*, 389–405.

Oyama, T., Shimura, Y., and Okada, K. (1997). The *Arabidopsis HY5* gene encodes a bZIP protein that regulates stimulus-induced development of root and hypocotyl. Genes Dev. *11*, 2983–2995.

Quail, P.H., Briggs, W.R., Chory, J., Hangarter, R.P., Harberd, N.P., Kendrick, R.E., Koornneef, M., Parks, B., Sharrock, R.A., Schäfer, E., et al. (1994). Spotlight on phytochrome nomenclature. Plant Cell *6*, 468–471.

Rockwell, N.C., Su, Y.S., and Lagarias, J.C. (2006). Phytochrome structure and signaling mechanisms. Annu. Rev. Plant Biol. *57*, 837–858.

Rösler, J., Klein, I., and Zeidler, M. (2007). Arabidopsis fhl/fhy1 double mutant reveals a distinct cytoplasmic action of phytochrome A. Proc. Natl. Acad. Sci. USA *104*, 10737–10742.

Schäfer, E. (1975). A new approach to explain the "high irradiance responses" of photomorphogenesis on the basis of phytochrome. J. Math. Biol. *2*, 41–56.

Schäfer, E., Lassig, T.U., and Schopfer, P. (1975). Photocontrol of phytochrome destruction in grass seedlings. The influence of wavelength and irradiance. Photochem. Photobiol. *22*, 193–202.

Schäfer, E., and Mohr, H. (1974). Irradiance dependency of the phytochrome system in cotyledons of mustard (*Sinapis alba* L.). J. Math. Biol. *1*, 9–15.

Shen, Y., Zhou, Z., Feng, S., Li, J., Tan-Wilson, A., Qu, L.J., Wang, H., and Deng, X.W. (2009). Phytochrome A mediates rapid red light-induced phosphorylation of Arabidopsis FAR-RED ELONGATED HYPOCOTYL1 in a low fluence response. Plant Cell *21*, 494–506.

Shinomura, T., Nagatani, A., Hanzawa, H., Kubota, M., Watanabe, M., and Furuya, M. (1996). Action spectra for phytochrome A- and B-specific photoinduction of seed germination in *Arabidopsis thaliana*. Proc. Natl. Acad. Sci. USA *93*, 8129–8133.

Shinomura, T., Uchida, K., and Furuya, M. (2000). Elementary processes of photoperception by phytochrome A for high-irradiance response of hypocotyl elongation in *Arabidopsis*. Plant Physiol. *122*, 147–156.

Sorokina, O., Kapus, A., Terecskei, K., Dixon, L.E., Kozma-Bognar, L., Nagy, F., and Millar, A.J. (2009). A switchable light-input, light-output system modelled and constructed in yeast. J. Biol. Eng. *3*, 15.

Su, Y.S., and Lagarias, J.C. (2007). Light-independent phytochrome signaling mediated by dominant GAF domain tyrosine mutants of Arabidopsis phytochromes in transgenic plants. Plant Cell *19*, 2124–2139.

von Dassow, G., Meir, E., Munro, E.M., and Odell, G.M. (2000). The segment polarity network is a robust developmental module. Nature *406*, 188–192.

Whitelam, G.C., Johnson, E., Peng, J., Carol, P., Anderson, M.L., Cowl, J.S., and Harberd, N.P. (1993). Phytochrome A null mutants of *Arabidopsis* display a wild-type phenotype in white light. Plant Cell *5*, 757–768.

Yang, S.W., Jang, I.C., Henriques, R., and Chua, N.H. (2009). FAR-RED ELONGATED HYPOCOTYL1 and FHY1-LIKE associate with the Arabidopsis transcription factors LAF1 and HFR1 to transmit phytochrome A signals for inhibition of hypocotyl elongation. Plant Cell *21*, 1341–1359.

Zeidler, M., Bolle, C., and Chua, N.-H. (2001). The phytochrome A specific signaling component PAT3 is a positive regulator of *Arabidopsis* photomorphogenesis. Plant Cell Physiol. *42*, 1193–1200.

Zhou, Q., Hare, P.D., Yang, S.W., Zeidler, M., Huang, L.-F., and Chua, N.-H. (2005). FHL is required for full phytochrome A signaling and shares overlapping functions with FHY1. Plant J. *43*, 356–370.